In liver fibrosis, dendritic cells govern hepatic inflammation in mice via TNF-α

Michael K. Connolly,[1] Andrea S. Bedrosian,[1] Jon Mallen-St. Clair,[2] Aaron P. Mitchell,[3] Junaid Ibrahim,[1] Andrea Stroud,[3] H. Leon Pachter,[1] Dafna Bar-Sagi,[2] Alan B. Frey,[3] and George Miller[1,3]

[1]S. Arthur Localio Laboratory, Department of Surgery, [2]Department of Biochemistry, and [3]Department of Cell Biology, New York University School of Medicine, New York, New York, USA.

Hepatic fibrosis occurs during most chronic liver diseases and is driven by inflammatory responses to injured tissue. Because DCs are central to modulating liver immunity, we postulated that altered DC function contributes to immunologic changes in hepatic fibrosis and affects the pathologic inflammatory milieu within the fibrotic liver. Using mouse models, we determined the contribution of DCs to altered hepatic immunity in fibrosis and investigated the role of DCs in modulating the inflammatory environment within the fibrotic liver. We found that DC depletion completely abrogated the elevated levels of many inflammatory mediators that are produced in the fibrotic liver. DCs represented approximately 25% of the fibrotic hepatic leukocytes and showed an elevated $CD11b^+CD8^-$ fraction, a lower $B220^+$ plasmacytoid fraction, and increased expression of MHC II and CD40. Moreover, after liver injury, DCs gained a marked capacity to induce hepatic stellate cells, NK cells, and T cells to mediate inflammation, proliferation, and production of potent immune responses. The proinflammatory and immunogenic effects of fibrotic DCs were contingent on their production of TNF-α. Therefore, modulating DC function may be an attractive approach to experimental therapeutics in fibro-inflammatory liver disease.

Introduction

DCs are professional APCs and initiate both innate and adaptive immunity. However, although DCs mediate powerful immune responses in most contexts, liver DCs have a distinctly tolerogenic phenotype. The propensity of liver DCs to initiate tolerogenic rather than immunogenic responses to antigen — by induction of Tregs or through active T cell deletion — is thought to be the basis of hepatic tolerance (1). Liver DCs contain robust numbers of $B220^+$ plasmacytoid cells, which are poor inducers of antigen-specific immunity (2). Xia et al. (3) recently showed that the unique hepatic microenvironment programs Lin^-CD117^+ hematopoietic progenitor differentiation into regulatory DCs responsible for maintaining liver tolerance. We have previously shown that, as a consequence of their immaturity and distinct subset composition, liver DCs are poorly immunogenic compared with spleen DCs (4). Goubier et al. (1) reported that liver DCs induce tolerance to oral antigen by active T cell deletion. Although normal liver DCs are poor initiators of immunity, the function of DCs in states of hepatic injury, such as liver fibrosis, has not previously been investigated.

Liver fibrosis is a leading cause of morbidity and mortality. Human and animal studies suggest that hepatic immunity is altered in fibrosis (5, 6) and that liver inflammation is the hallmark of early-stage liver fibrosis, ultimately resulting in hepatic stellate cell (HSC) activation and ECM deposition. In particular, various immunoregulatory cytokines and chemokines, including TNF-α, IL-6, MIP-1α, MIP-1β, and RANTES, are critical mediators in fibrosis (7, 8). Because DCs are central to modulating liver immunity (9), we postulated that a transformation of DC function from tolerogenic to immunogenic underlies the immunologic and inflammatory changes in liver fibrosis. We found that hepatic DCs expanded 5-fold in liver fibrosis and acquired an activated surface phenotype and the marked ability to stimulate NK cells, T cells, and HSCs in a TNF-α–dependent manner. Moreover, DCs govern the hepatic inflammatory milieu, as DC depletion abrogated the cytokine and chemokine environment distinctive of hepatic fibrosis. Our findings offer a critical understanding of immunity and inflammation in liver fibrosis.

Results

Models of fibrosis. Mice treated for 6 weeks with thioacetamide (TAA) and leptin demonstrated micronodular fibrosis on morphologic examination (Figure 1A). Treated mice exhibited slightly retarded weight gain (Supplemental Figure 1A; supplemental material available online with this article; doi:10.1172/JCI37581DS1) and increased susceptibility to bacterial LPS (Supplemental Figure 1B), but had no evidence of ascites or gastrointestinal varices (data not shown). Mice did not develop primary liver cancer even after 6 months of treatment. Histologic analysis revealed that in treated animals, the organized hepatic architecture was replaced by regenerative nodules bounded by fibrous septa (Figure 1B). Diffuse biliary ductal proliferation and a mild lymphocytic infiltrate were also evident in fibrotic livers. Biochemical analysis of serum from treated animals revealed elevations in liver enzymes consistent with a fibrotic phenotype (Supplemental Figure 2). Similar features were seen using the CCl_4 model (data not shown).

The composition of hepatic nonparenchymal cells is altered in the fibrotic liver. On average, approximately 1×10^7 nonparenchymal cells (NPCs) were isolated from both fibrotic and normal mouse livers. However, the cellular composition of NPCs was vastly different in fibrotic animals. In particular, $CD11c^+$ DCs were expanded from a baseline of approximately 5% of NPCs in normal mice to 20%–27% in fibrotic

Authorship note: Michael K. Connolly and Andrea S. Bedrosian are co-first authors and contributed equally to this work.

Conflict of interest: The authors have declared that no conflict of interest exists.

Citation for this article: *J. Clin. Invest.* **119**:3213–3225 (2009). doi:10.1172/JCI37581.

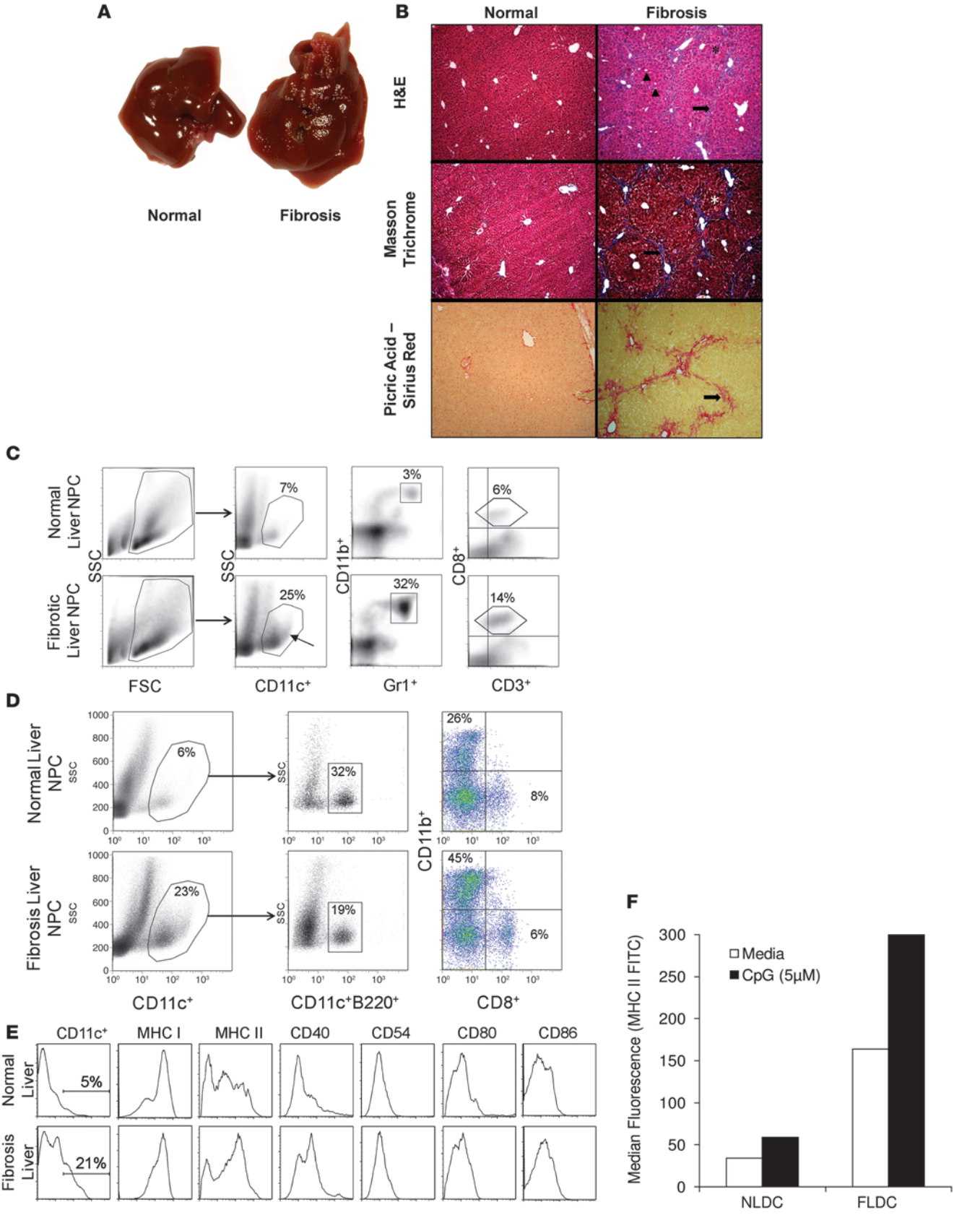
A
Normal
Fibrosis
B
Normal
Fibrosis
H&E
Masson Trichrome
Picric Acid – Sirius Red
C
Normal Liver NPC
Fibrotic Liver NPC
SSC
FSC
7%
25%
CD11c+
3%
32%
Gr1+
CD11b+
6%
14%
CD3+
CD8+
D
Normal Liver NPC
Fibrosis Liver NPC
SSC
6%
23%
CD11c+
32%
19%
CD11c+B220+
26%
8%
45%
6%
CD11b+
CD8+
E
CD11c+
MHC I
MHC II
CD40
CD54
CD80
CD86
Normal Liver
Fibrosis Liver
5%
21%
F
Median Fluorescence (MHC II FITC)
Media
CpG (5μM)
NLDC
FLDC

Figure 1
Hepatic fibrosis alters the composition of liver NPC and DC phenotype. (**A**) The liver surface contour of TAA/leptin-treated mice was markedly irregular. (**B**) H&E examination of the livers of treated mice revealed a distorted hepatic architectural pattern. Regenerative nodules were seen (asterisks), bounded by fibrous septa (arrows). In addition, there was diffuse ductal proliferation (arrowheads). Masson trichrome and picric acid–Sirius red staining highlighted the collagen network surrounding and bridging the portal triads. Original magnification, ×10 (H&E and Masson trichrome); ×20 (picric acid–Sirius red). (**C**–**E**) Liver NPCs were analyzed by flow cytometry. The percentage of cells within selected gates is indicated. (**C**) Density plots of NPCs from normal and fibrotic liver. $CD11c^+$ DCs increased in fibrotic livers. In addition, a $CD11c^{hi}$ subpopulation expanded in fibrotic livers (arrow), which was rare in controls. $Gr1^+CD11b^+$ myeloid-derived cells and $CD3^+CD8^+$ T cells were also dramatically expanded in fibrotic livers. (**D**) DC subset analysis revealed a lower $CD11c^+B220^+$ plasmacytoid fraction and a higher $CD11b^+CD8^-$ fraction among FLDCs compared with NLDCs. (**E**) Liver $CD11c^+$ cells were assayed for expression of DC surface markers. Histograms show that freshly isolated FLDCs were more mature than controls. (**F**) FACS-sorted $CD11c^+$ DCs were cultured for 24 hours either alone or with supplemental CpG before analysis for MHC II expression by flow cytometry. Median fluorescence is shown. There was considerably higher MHC II expression in FLDCs compared with NLDCs ($P < 0.05$). Isotype staining was similar for both groups (not shown). Phenotypic studies were repeated 4 times.

mouse livers (Figure 1C). In addition, a distinct $CD11c^{hi}$ population was present in fibrotic livers that was rare in normal liver. The total number of DCs increased from approximately 2–4 × 10^5 in normal livers to 1–3 × 10^6 in fibrotic livers (Supplemental Figure 3). Similarly, $Gr1^+CD11b^+$ myeloid cells expanded from less than 5% in normal livers to 30% in mice with liver fibrosis (Figure 1C). In addition, $CD3^+CD8^+$ T cells represented only 3%–6% of NPCs in normal murine livers, but increased to 8%–14% in mice with fibrosis. Conversely, the percentage of liver $CD3^+CD4^+$ T cells was consistently more than 2-fold lower in fibrotic livers (data not shown), as was the subfraction of hepatic $CD4^+CD25^+Foxp^+$ Tregs (Supplemental Figure 4). However, in contrast to the altered liver NPC composition, the splenocyte composition was unchanged in fibrotic mice, and there was no expansion of the splenic DC population (Supplemental Figure 5), which indicates that the effects are liver specific.

DCs in fibrotic liver have a distinct phenotype. In addition to their increased number, DCs from fibrotic liver (FLDCs) exhibited a distinct phenotype indicative of enhanced maturity. $CD11b^+CD8^-$ myeloid DCs were about 20% higher, and $B220^+$ plasmacytoid DCs about 15% lower, among FLDCs compared with normal liver DCs (NLDCs; Figure 1D). Nevertheless, the absolute number of plasmacytoid DCs was higher in fibrotic mice as a result of the overall expansion of the DC compartment. We did not observe any change in the fraction of $NK1.1^+CD11c^+$ cells (data not shown). FLDCs were also more mature than NLDCs (Figure 1E). In particular, MHC II and CD40 expression, both critically associated with antigen presentation, were upregulated in FLDCs. Differences in MHC II expression levels between FLDCs and NLDCs were even more pronounced after 24 hours of culture (Figure 1F).

FLDCs produce elevated TNF-α and IL-6. Because FLDCs had an activated surface phenotype, we postulated that they would produce elevated levels of immunoregulatory cytokines. After 24 hours of culture, FLDCs from TAA/leptin-treated mice produced more than a 2-fold increase in both TNF-α and IL-6 compared with NLDCs (Figure 2, A and B). Similar effects were seen in the CCl_4 model (data not shown). TLR9 ligation with CpG enhanced TNF-α and IL-6 production in both FLDCs and NLDCs (Figure 2, A and B). Surprisingly, however, stimulation with the TLR3 ligand Poly(I:C), the TLR4 ligand LPS, or the TLR5 ligand Flagellin did not increase production of TNF-α (Figure 2A) or IL-6 (data not shown).

DCs are the primary determinants of the cytokine milieu in the fibrotic liver. Because both IL-6 and TNF-α have pleiotropic effects on hepatic leukocytes in liver fibrosis (10, 11), we postulated that DCs may be a central determinant of the inflammatory milieu in the fibrotic liver. To test this hypothesis, NPCs were harvested from normal and fibrotic livers and cultured for 24 hours without exogenous stimulation in parallel with NPCs from fibrotic livers that had been depleted of DCs. Inflammatory mediators important in fibro-inflammatory liver disease (12) were quantitated in conditioned media. NPCs from fibrotic liver produced up to 100-fold elevations in several cytokines and chemokines compared with normal NPCs (Figure 2, C–E). However, DC depletion from fibrotic NPC cultures completely eliminated the elevated production of soluble inflammatory mediators (Figure 2, C–E). While direct DC secretion of TNF-α and IL-6 may be responsible, at least in part, for reduced levels of these cytokines upon DC depletion, considering that FLDCs alone did not produce elevated levels of any of the other cytokines or chemokines tested (either immediately upon harvest from fibrotic liver or after 24 hours of NPC culture), these data suggest that DCs secondarily account for the markedly elevated inflammatory environment in fibrotic liver cultures by activation of neighboring cell types.

To determine whether in vivo DC depletion in fibrotic mice also decreases production of inflammatory mediators by liver leukocytes, CD11c-DTR mice were made fibrotic using TAA/leptin before depletion of DCs in vivo for 48 hours before sacrifice. Again, DC depletion markedly diminished the elevated cytokine and chemokine production by fibrotic NPCs (Figure 2F).

FLDCs are powerful stimulants of NK cell cytokine production and cytolysis. To determine the mechanism of DC augmentation of the inflammatory milieu after hepatic injury, we studied the interactions of FLDCs with immune effector cells. Because DC production of TNF-α can have powerful effects on innate immunity (13), we postulated that FLDCs may induce NK cell cytotoxicity and cytokine secretion. To test this, we cocultured FLDCs and NLDCs with normal splenic NK cells. After 24 hours, NK cells were repurified and assayed for cytotoxicity. NK cells harvested from coculture with NLDCs produced minimal lysis of Yac-1 targets. Conversely, coculture with FLDCs produced highly lytic NK cells (Figure 3A). To determine whether the enhanced NK cell activation by FLDCs is related to their production of TNF-α, we blocked TNF-α activity using a mAb. TNF-α blockade abrogated the marked NK-mediated cytolysis induced by FLDCs (Figure 3A), which suggests that elevated production of TNF-α mediates NK cell activation.

To determine whether cross-talk between DCs and NK cells may also contribute to the elevated inflammatory environment in fibrotic livers, we measured the levels of a number of immune-regulatory cytokines and chemokines produced in DC-NK coculture. NK cells cultured with FLDCs produced more than 700 pg/ml of TNF-α, compared with 100 pg/ml for FLDCs cultured alone and undetectable levels (<7 pg/ml) produced by NK cells alone. In contrast, NLDCs in coculture with NK cells did not enhance secretion of TNF-α (Figure 3B). FLDCs also stimulated NK cells to produce modest levels of IFN-γ, but NLDCs did not (Figure 3C). In consort with the notion that NK activation by FLDCs results from high-

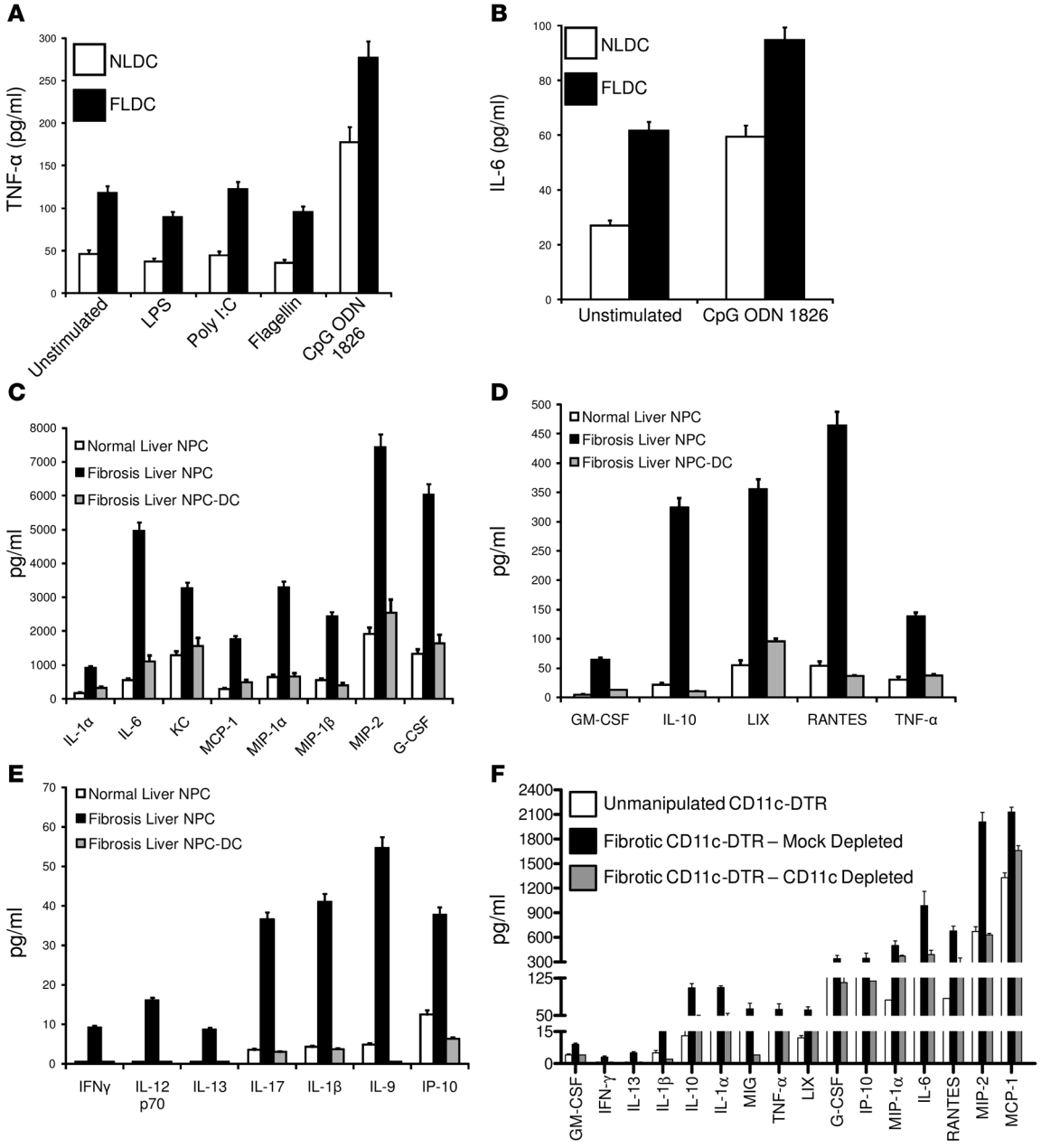

Figure 2

DCs control the inflammatory milieu in liver fibrosis. (**A**) Freshly isolated liver DCs were cultured for 24 hours at a concentration of 1×10^6. FLDCs produced more than 2-fold elevation in TNF-α compared with controls ($P < 0.05$). TNF-α production was further enhanced as a result of TLR9 ligation, but not TLR3, TLR4, or TLR5 ligation. (**B**) Similarly, FLDCs also produced elevated levels of IL-6 ($P < 0.05$). (**C**–**E**) NPCs were harvested from the livers of normal and fibrotic mice and cultured for 24 hours at a concentration of 1×10^6. Depletion of DCs from fibrotic NPC concentrates by FACS abrogated their elevated cytokine and chemokine production ($P < 0.05$ for each inflammatory mediator). (**F**) Freshly isolated NPCs from unmanipulated CD11c-DTR mice, fibrotic CD11c-DTR mice, or fibrotic CD11c-DTR mice that were depleted of DCs for 48 hours immediately prior to sacrifice were cultured as above. Cell culture supernatant was then assayed for inflammatory mediators. DC depletion in vivo in fibrotic mice markedly decreased NPC cytokine and chemokine production ($P < 0.05$ for each inflammatory mediator).

er DC production of TNF-α, blockade of TNF-α reduced IFN-γ production nearly 4-fold (Figure 3C). Moreover, FLDCs induced markedly high MCP-1, IL-6, and IL-10 production in coculture with NK cells, whereas NLDCs were nonactivating (Figure 3, D and E). Again, this production was partially reduced by TNF-α blockade. Similarly, NK coculture with FLDCs — but not NLDCs — resulted in markedly elevated production of IL-2, IP-10, GM-CSF, MIP-1β, MIP-2, and RANTES in a TNF-α–dependent manner (data not shown). Taken together, these data suggest that that DCs can modulate the hepatic cytokine and chemokine milieu in fibrosis, beyond their own production of TNF-α and IL-6, by NK activation via a mechanism that is, at least in part, TNF-α dependent.

Because TNF-α production by FLDCs was augmented by TLR9 ligation (Figure 2A), we postulated that CpG may enable FLDCs to further activate NK cells. Addition of 5 μM CpG to FLDC-NK cocultures increased NK cell IFN-γ production more than 20-fold (Figure 3F). Conversely, TLR9 ligation of NLDCs did not increase their ability to activate NK cells (Figure 3F and Supplemental Figure 6). Similarly, CpG differentially enhanced IL-6 production in FLDC-NK coculture wells (Figure 3G). These data suggest that in liver fibrosis, DCs become disproportionately activated and enabled to engage innate immunity as a result of TLR9 ligation.

FLDCs activate NK cells in vivo. Using adoptive transfer models, we next investigated whether FLDCs induce NK cell activity in vivo. $CD11c^+$ DCs were harvested from normal or fibrotic liver and incubated with CpG ODN 1826 before adoptive transfer to naive mice by direct splenic inoculation. At 18 hours, splenic NK cells were isolated and assayed for production of a select number of cytokines. NK cells from mice inoculated with FLDCs produced 3- to 10-fold higher levels of IFN-γ and IL-6 than did mice inoculated with NLDCs or saline (Figure 4A). Moreover, NK cells produced very robust levels of MCP-1 after in vivo inoculation with FLDCs (Figure 4B). We also investigated whether FLDCs induce enhanced NK cell production of chemokines in vivo using the same experimental strategy. FLDC inoculation resulted in 2-fold elevations in NK production of MIP-1α and MIP-1β (Figure 4, B and C), as well as MIP-2 and RANTES (data not shown). In keeping with their ability to activate NK function in vivo, adoptive transfer of CpG-primed FLDCs differentially upregulated CD69 expression on splenic NK cells compared with the effects of NLDCs (Figure 4D). These data highlight the capacity of DCs from fibrotic liver to activate NK cells in vivo and thereby modulate the inflammatory milieu.

Immunization with antigen-pulsed FLDCs induces a markedly elevated CTL response. Because FLDCs governed the elevated hepatic inflammatory milieu in fibrosis (Figure 2, C–F) and markedly activated NK cells (Figures 3 and 4), we postulated that FLDCs may also differentially engage adaptive immunity in vivo and generate cytotoxic T cells. To test this, naive C57BL/6 mice were immunized with adoptively transferred NLDCs and FLDCs pulsed with $Ova_{257–264}$ peptide (NLDC.$Ova_{257–264}$ and FLDC.$Ova_{257–264}$, respectively) before assay of Ova-specific cytolysis in vitro. Restimulated splenocytes from mice immunized with NLDC.$Ova_{257–264}$ produced virtually no target lysis, consistent with the tolerogenic immunophenotype of NLDCs. However, splenocytes from mice immunized with FLDC.$Ova_{257–264}$ produced nearly 40% target lysis at the highest effector/target (E/T) ratio and maintained substantial lytic ability even at low E/T ratios (Figure 5A). Immunization with adoptively transferred spleen DC.$Ova_{257–264}$ from fibrotic mice produced a much smaller increase in target lysis compared with normal spleen DC.$Ova_{257–264}$ (Figure 5B).

To further explore the immunogenicity of DCs in liver fibrosis and their modulation of the inflammatory milieu, we investigated whether immunization with antigen-pulsed FLDCs induces Th1 or Th2 cytokine elaboration. To test this, supernatant was harvested from the CTL cultures in the above experiments and assayed. We found that CTL cultures from mice immunized with antigen-pulsed FLDCs produced very high levels of IFN-γ. In contrast, IFN-γ levels were minimal in CTL cultures from mice immunized with saline or antigen-loaded NLDCs (Figure 5C). In addition, CTL cultures from mice immunized with FLDC.$Ova_{257–264}$ produced highly elevated levels of the Th2 cytokines IL-10 (Figure 5D) and IL-5 (Figure 5E). Taken together, our data suggest that both Th1 and Th2 mechanisms are activated by antigen-pulsed FLDCs, whereas NLDCs are relatively inert.

Antigen-loaded FLDCs produce enhanced $CD4^+$ and $CD8^+$ T cell proliferation in draining lymph nodes and in the liver. To further assess the immunogenicity of FLDCs, we tested their capacity to migrate to regional lymph nodes and prime antigen-restricted $CD4^+$ T cells. $CD45.1^+$ congenic mice were adoptively transferred with $CD45.2^+CD4^+$OT-II T cells followed 18 hours later by footpad inoculation with DC.$Ova_{323-339}$. At 90 hours, ipsilateral popliteal lymph nodes were harvested, and the fraction of $CD4^+CD45.2^+$ T cells was determined by flow cytometry. FLDCs induced substantial antigen-specific $CD4^+$ T cell proliferation in the draining nodal basin, while NLDCs were minimally stimulatory (Figure 6A). Furthermore, FLDCs induced marked T cell activation (as determined by CD25 expression) compared with NLDCs (Figure 6A).

To test the capacity of antigen-pulsed FLDCs to induce $CD8^+$ T cell proliferation in vivo, a similar adoptive transfer model was used. Mice were administered $CD8^+$OTI T cells followed 18 hours later by i.v. inoculation with DC.$Ova_{257–264}$. At 90 hours, liver NPCs were harvested, and the fraction of $CD8^+Ova_{257–264}$Pentamer$^+$ T cells was determined by flow cytometry. In concert with our previous findings, antigen-pulsed FLDCs induced higher $CD8^+$ T cell proliferation in vivo (Supplemental Figure 7). Taken together, our data suggest that, although DCs from normal liver are poorly immunogenic, DCs from fibrotic liver are potent APCs.

Cross-presentation of antigen in the liver has recently been shown to be mediated by liver DCs (9). Because FLDCs have enhanced capacity to stimulate T cells in vivo, we postulated that cross-presentation would be enhanced in situ within the fibrotic liver. To test this, normal and fibrotic mice were adoptively transferred with OT-I T cells followed by i.v. administration of Ova 18 hours later. On day 4, the number of liver $CD8^+Ova_{257–264}$Pentamer$^+$ T cells was measured. Cross-presentation in the fibrotic liver was more vigorous than in the normal liver (Figure 6B).

FLDCs induce enhanced T cell stimulation by a TNF-α–dependent mechanism. We postulated that, similar to our DC-NK findings, TNF-α may be responsible for the enhanced capacity of FLDCs to activate T cells. To test this, we used in vitro models. Antigen-specific $CD4^+$ T cell stimulation was evaluated by plating irradiated DC.$Ova_{323-339}$ with $CD4^+$ OT-II T cells. Consistent with our in vivo data, FLDCs induced higher OT-II proliferation than did NLDCs (Figure 6C); however, TNF-α blockade abrogated the higher OT-II proliferation (Figure 6D). To measure DC induction of antigen-restricted $CD8^+$ T cells in vitro, DCs were loaded with $Ova_{257–264}$ and then used to stimulate $CD8^+$ OT-I T cells. Again, DCs from the livers of fibrotic mice induced higher OT-I proliferation than did NLDCs (Figure 6E), and TNF-α blockade reduced OT-I proliferation to baseline (Figure 6F). Taken together, our data suggest that TNF-α is responsible, at least in part, for the enhanced ability of FLDCs to engage adaptive immunity.

FLDCs differentially enhance T cell phenotype. To further investigate the immunogenic capacity of DCs from fibrotic animals, we analyzed their ability to induce an activated T cell surface phenotype. Liver and spleen DCs from normal and fibrotic C57BL/6 mice were cocultured with allogeneic T cells from BALB/c mice before determination of T cell surface phenotype by flow cytometry. Compared with NLDCs, FLDCs differentially downregulated CD62L expression and upregulated CD11b and CD178 expression on allogeneic T cells. Conversely, spleen DCs from fibrotic mice minimally enhanced T cell surface phenotype compared with

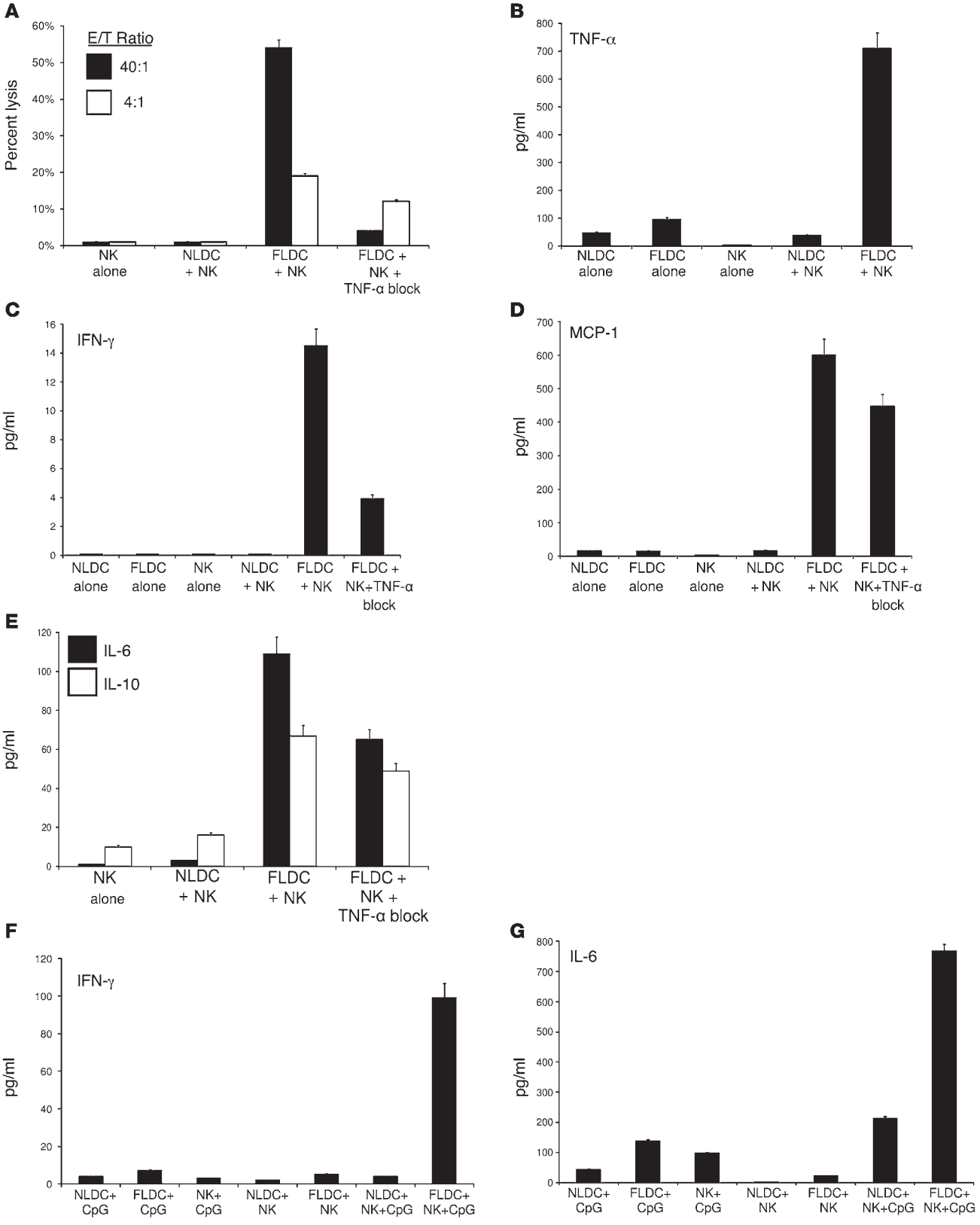
A
Percent lysis
E/T Ratio
40:1
4:1
NK alone
NLDC + NK
FLDC + NK
FLDC + NK + TNF-α block
B
TNF-α
pg/ml
NLDC alone
FLDC alone
NK alone
NLDC + NK
FLDC + NK
C
IFN-γ
pg/ml
NLDC alone
FLDC alone
NK alone
NLDC + NK
FLDC + NK
FLDC + NK+TNF-α block
D
MCP-1
pg/ml
NLDC alone
FLDC alone
NK alone
NLDC + NK
FLDC + NK
FLDC + NK+TNF-α block
E
IL-6
IL-10
pg/ml
NK alone
NLDC + NK
FLDC + NK
FLDC + NK + TNF-α block
F
IFN-γ
pg/ml
NLDC+ CpG
FLDC+ CpG
NK+ CpG
NLDC+ NK
FLDC+ NK
NLDC+ NK+CpG
FLDC+ NK+CpG
G
IL-6
pg/ml
NLDC+ CpG
FLDC+ CpG
NK+ CpG
NLDC+ NK
FLDC+ NK
NLDC+ NK+CpG
FLDC+ NK+CpG

Figure 3
Liver DCs from fibrotic mice induce elevated NK cell–mediated cytotoxicity in vitro via production of TNF-α. (**A**) NLDCs or FLDCs were cocultured with splenic NK cells for 24 hours in a 2:1 DC/NK ratio. NK cells were then repurified and plated against ^{51}Cr-labeled Yac-1 lymphoma targets. NK cells cocultured with DCs from fibrotic livers produced markedly high Yac-1 lysis, which was TNF-α dependent, whereas NK cells cultured alone or cocultured with NLDCs induced virtually no target lysis ($P < 0.05$). (**B**–**E**) Analysis of cytokine production from DC-NK coculture revealed that FLDCs induced elevated production of (**B**) TNF-α, (**C**) IFN-γ, (**D**) MCP-1, and (**E**) IL-6 and IL-10 ($P < 0.05$). However, in each case, TNF-α blockade partially abrogated the elevated cytokine production ($P < 0.05$). Addition of 5 μM CpG to FLDC-NK coculture wells further markedly enhanced production of (**F**) IFN-γ and (**G**) IL-6 ($P < 0.05$). DC-NK coculture assays were repeated 4 times with similar results.

normal spleen DCs (Figure 7A). In addition to inducing a more activated T cell phenotype, FLDCs induced nearly 2-fold higher T cell proliferation in a mixed lymphocyte reaction (MLR) compared with NLDCs (Figure 7B). Conversely, splenic DCs from fibrotic mice did not induce augmented alloproliferation compared with controls (Figure 7C), again suggesting that heightened immunogenicity of DCs in fibrosis is liver specific.

Immunization with FLDCs prevents tumor growth. The accumulated data suggest that the tolerogenic properties of liver DCs are reversed to potent immunogenicity in fibrosis. To test this further, we examined the capacity of liver DCs to protect against tumor development. DCs were harvested from the livers of normal or fibrotic mice, loaded with $Ova_{257-264}$, incubated with CpG, and then adoptively transferred to naive mice. Immunization was repeated again on day 7, before s.c. tumor challenge on day 14 with EG7 cells. All mice immunized with saline or NLDC.$Ova_{257-264}$ showed tumor development by day 11 after challenge. Conversely, mice immunized with FLDC.$Ova_{257-264}$ were completely protected from tumor development (Figure 7D). Immunization with mock-loaded FLDCs did not protect against EG7 (data not shown).

FLDCs directly induce HSCs. Because quiescent HSCs transform into proinflammatory mediators after hepatic injury (12), we sought to determine whether DCs directly engage HSCs. Freshly isolated NLDCs or FLDCs were cocultured with HSCs from normal liver. After 24 hours, the nonadherent DCs were washed off, and the HSCs were either immediately analyzed by flow cytometry or cultured alone for an additional 24 hours. FLDCs induced increased expression of ICAM-1 and CD40 on HSCs (Figure 8A). Moreover, HSCs that had been simulated by FLDCs produced marked elevations in variety of cytokines (i.e., IL-1α, IL-6, G-CSF, GM-CSF, IL-13, LIF, and MCP-1) and chemokines (i.e., MIP-1α, MIP-1β, MIP-2, KC, and MIG) characteristically elevated during the early inflammatory phase of liver fibrosis (Figure 8, B and C, and ref. 12). Conversely, NLDCs were minimally activating to HSCs. Furthermore, consistent with our earlier findings (Figure 3, F and G), TLR9 ligation of DCs prior to HSC coculture markedly enhanced the capacity of FLDCs to induce HSCs to produce IL-1α, IL-6, G-CSF, GM-CSF, MIG, and MCP-1. In contrast, TLR9 ligation of NLDCs failed to augment their ability to activate HSCs (Figure 8, B and C).

Because TNF-α was required for FLDCs to optimally engage NK and T cells, we postulated that TNF-α may also be important for FLDCs to activate HSCs. In addition, we wanted to determine whether direct cellular contact is needed for FLDCs to induce HSCs or whether FLDC secretions alone are sufficient for HSC activation. To explore these questions, we repeated the FLDC-HSC coculture experiments, but used both transwell inserts to separate DCs from contact with HSCs and an anti–TNF-α mAb. We

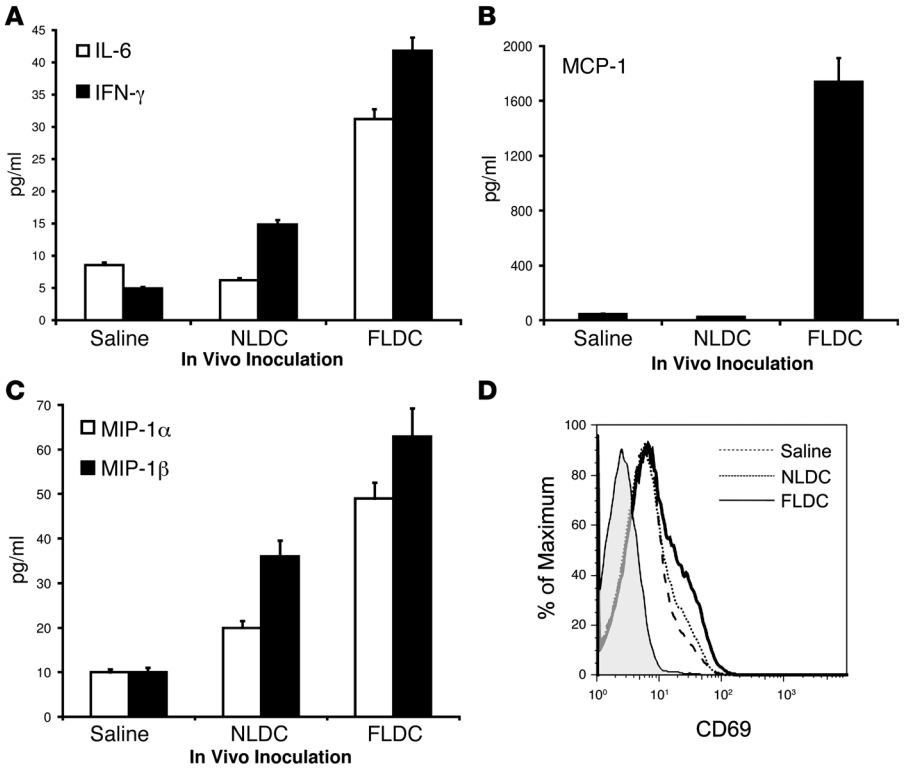

Figure 4
Adoptive transfer of DCs from livers of fibrotic mice activates NK cells in vivo. DCs (1×10^5) were harvested from the livers of normal or fibrotic mice by FACS, incubated for 6 hours with 5 μM CpG, and then injected directly into the spleens of naive animals. At 18 hours, NK cells were harvested from the spleens of recipient mice, plated at a concentration of 1×10^6, and assayed for production of (**A**) IL-6 and IFN-γ, (**B**) MCP-1, and (**C**) MIP-1α and MIP-1β in 24-hour cultures. (**A**–**C**) NK cells harvested from mice that received adoptively transferred FLDCs produced elevated IFN-γ, IL-6, MCP-1, MIP-1α, and MIP-1β (all $P < 0.05$). (**D**) Alternatively, NK cells from recipient mouse spleens were analyzed for CD69 expression by flow cytometry. CD69 was expressed at modestly higher levels on NK cells harvested from spleens injected with FLDCs compared with controls. The shaded histogram represents isotype staining. Experiments were repeated 3 times with similar results.

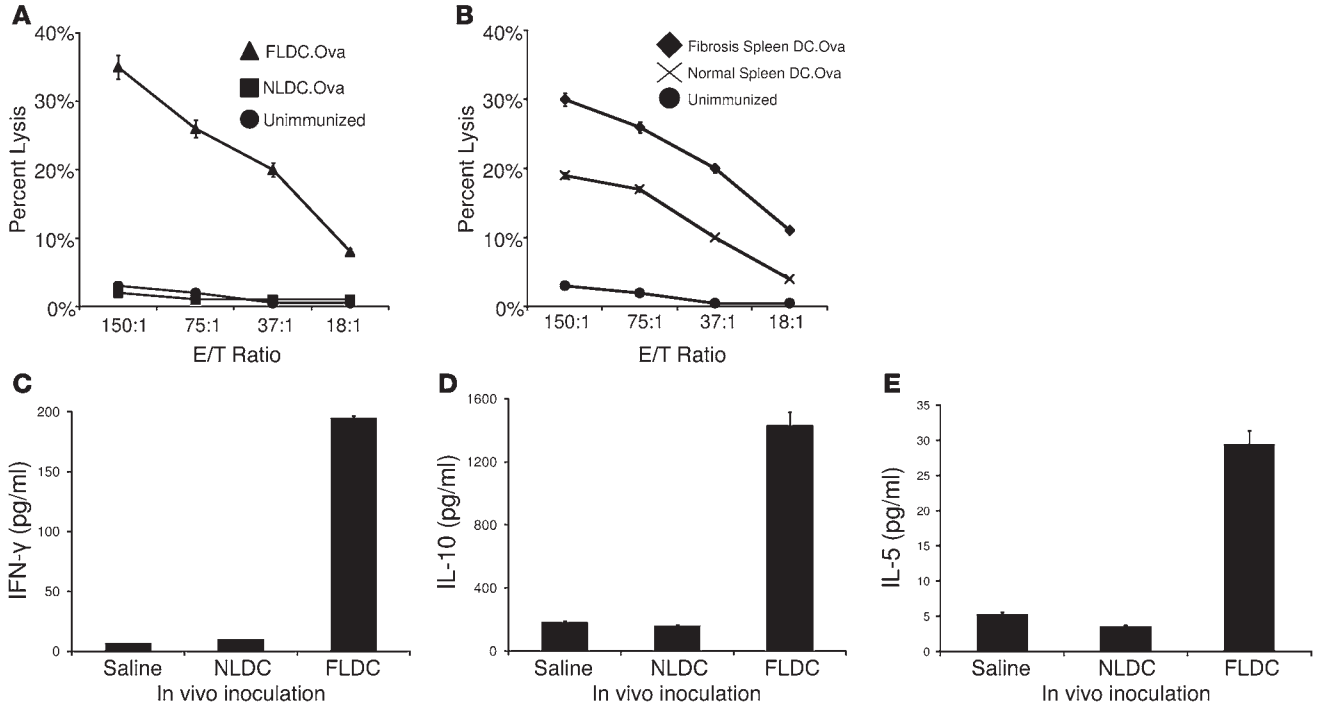

Figure 5

FLDCs have enhanced capacity to induce antigen-specific CTL lysis. Mice were immunized twice at weekly intervals with $Ova_{257–264}$ peptide-pulsed (**A**) liver or (**B**) spleen DCs from normal or fibrotic mice. At 1 week after the second immunization, splenocytes from immunized mice were harvested and restimulated for 5 days with $Ova_{257-264}$ peptide before assay of their lytic function using ^{51}Cr-labeled EG7 targets. (**A**) Immunization with $FLDC.Ova_{257–264}$, but not $NLDC.Ova_{257–264}$, produced marked CTL lysis ($P < 0.05$). (**B**) Immunization using antigen-loaded splenic DCs from fibrotic mice produced a modest benefit in CTL lysis compared with normal splenic DCs ($P < 0.05$). (**C**–**E**) Analysis of day-4 CTL cultures revealed that (**C**) IFN-γ, (**D**) IL-10, and (**E**) IL-5 were markedly elevated in CTL supernatant after immunization with $FLDC.Ova_{257-264}$ compared with controls (all $P < 0.05$). CTL experiments were repeated 3 times with similar results.

again found that FLDCs were efficient at inducing cytokine and chemokine production from HSCs (Figure 8D). However, TNF-α blockade during FLDC-HSC coculture partially reduced subsequent HSC production of IL-1α, IL-6, G-CSF, MIP-1β, MIP-2, and KC. Moreover, prevention of direct cell contact in FLDC-HSC cocultures markedly reduced the levels of inflammatory mediator production by HSCs. The combination of TNF-α blockade and prevention of cellular contact reduced the activating effects of FLDCs on HSCs even further (data not shown). These data imply that both direct cellular contact and well as secreted elements, including TNF-α, enable FLDCs to activate HSCs.

We also investigated whether liver DCs in fibrosis could induce the proliferation of HSCs, a hallmark of chronic fibro-inflammatory liver disease (12). Irradiated DCs were coincubated with HSCs for 48 hours. HSC proliferation was measured by uptake of ^{3}H-thymidine. Remarkably, FLDCs induced a 6-fold increase in HSC proliferation over baseline, whereas NLDCs had a weak proliferative effect (Figure 8E).

Discussion

One the most intriguing findings of this study was the marked enhancement of DC immunogenicity in fibrosis. FLDCs provided vigorous allogeneic and antigen-specific $CD4^+$ and $CD8^+$ T cell stimulation and efficient cross-presentation, generated an activated T cell surface phenotype, induced potent CTL responses, and induced an activated NK cell phenotype and high cytotoxicity. In all of the above assays, NLDCs were nonstimulatory. The heightened immunogenicity of FLDCs is underscored by our finding that adoptive transfer immunization using antigen-pulsed FLDCs protected 100% of mice from tumor challenge, whereas NLDCs were nonprotective (Figure 7D). The immunogenicity of liver DCs in fibrosis is related, at least in part, to their secretion of TNF-α. Other distinct characteristics of FLDCs, including their increased phenotypic maturation and heightened responsiveness to biologic stimuli such as TLR9 ligation, likely further contribute to their enhanced immunostimulatory capacity. Furthermore, in fibrotic animals, the phenotypic subsets of DCs also change to an immunogenic profile, including an increase in the $CD11b^+CD8^-$ fraction as well as a decrease in the proportion of $B220^+$ plasmacytoid DCs. We also found a sharp rise in $CD8^+$ T cells among fibrotic liver NPCs and a reduction in $CD4^+CD25^+Foxp^+$ Tregs, which may contribute to further enhanced liver immunogenicity in situ in fibrosis. The relevance of these findings to cirrhosis in humans is important. A recent report found that human liver DCs are composed primarily of BDCA-1 and BDCA-3 subsets and, similar to their murine counterparts, induce tolerogenic T cells responses to antigen and the expansion of Tregs (14). Further work is required in order to characterize the changes in human liver DCs in cirrhosis. However, this endeavor is encumbered by the fact that the majority of cirrhotic patients are coinfected with Hepatitis B or C, which alone alters DC immunophenotype (15, 16).

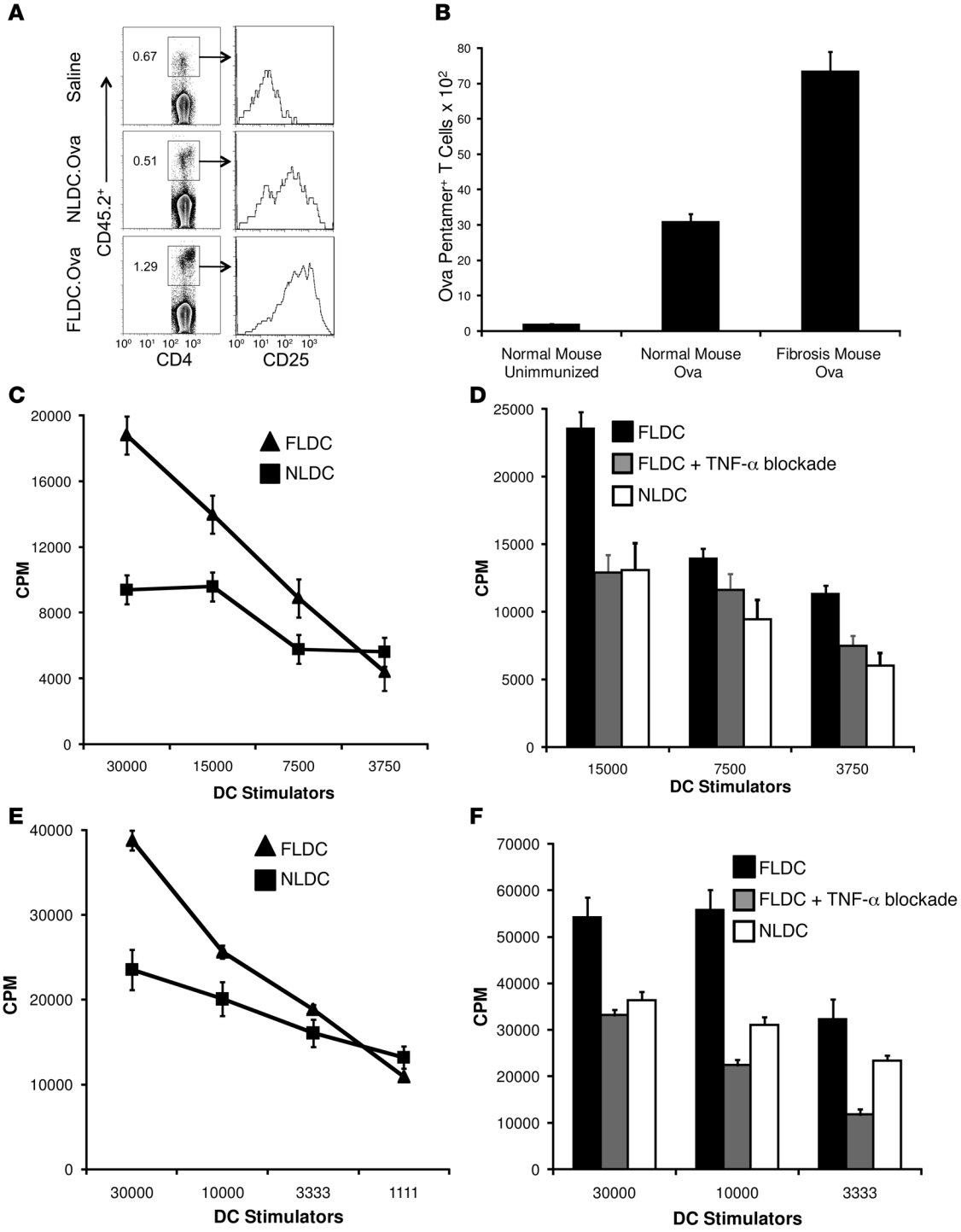

Figure 6

FLDCs have increased capacity to prime T cells. (**A**) To test the capacity of DCs to prime $CD4^+$ T cells in vivo, congenic $CD45.1^+$ mice were administered OT-II T cells (2×10^6) i.v. At 18 hours, recipient mice received footpad inoculations with $DC.Ova_{323–339}$ (2×10^5). At 90 hours, the percentage of $CD3^+CD4^+CD45.2^+$ T cells among all $CD3^+CD4^+$ T cells in draining popliteal lymph nodes (numbers within plots) and their expression of CD25 was determined. (**B**) To assess cross-presentation in situ, normal or fibrotic mice were administered 2×10^6 OT-I T cells followed by inoculation with 1 mg Ova at 18 hours. The number of hepatic $CD3^+CD8^+Ova_{257–264}Pentamer^+$ cells was measured at 90 hours. Cross-presentation was higher in the fibrotic liver ($P < 0.05$). (**C**) To test the capacity of FLDCs to prime antigen-restricted $CD4^+$ T cells in vitro, DCs were loaded with $Ova_{323–339}$ and used to stimulate OT-II T cells. Antigen-pulsed FLDCs induced higher OT-II T cell proliferation compared with NLDCs ($P < 0.05$ at the 3 highest concentrations). (**D**) However, TNF-α blockade abrogated the enhanced proliferation ($P < 0.05$). (**E**) Similarly, $FLDC.Ova_{257–264}$ induced more vigorous proliferation of OT-I T cells compared with $NLDC.Ova_{257–264}$ ($P < 0.05$ at the 2 highest concentrations). (**F**) Again, the enhanced $CD8^+$ T cell proliferation was abrogated by TNF-α blockade ($P < 0.05$). Assays were repeated at least 3 times with similar results.

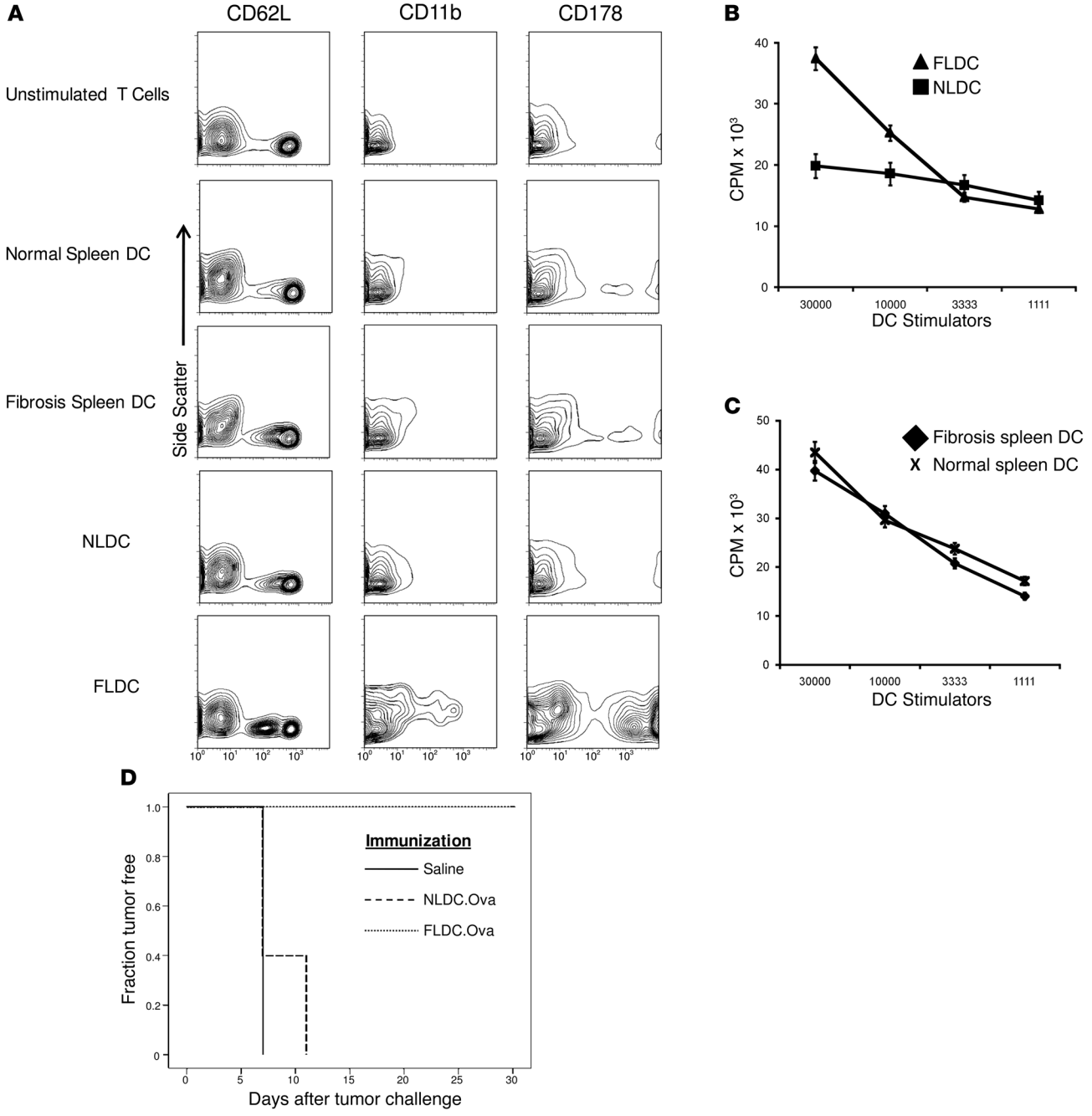

Figure 7

FLDCs activate T cells and can mediate tumor protection. (**A**) DCs (3×10^4) from C57BL/6 mice were cocultured with allogeneic BALB/c T cells (2×10^5) for 24 hours. $CD3^+$ T cells were then analyzed by flow cytometry. (**B**) FLDCs or NLDCs from C57BL/6 mice were plated with BALB/c T cells for 72 hours in an MLR before pulsing with ^{3}H-thymidine. FLDCs induced nearly twice the T cell proliferation than that of NLDCs at the 2 highest concentrations tested ($P < 0.05$). (**C**) Conversely, splenic DCs from fibrotic mice performed similar to normal spleen DCs. (**D**) To test the capacity of liver DCs to mediate tumor protection in vivo, naive mice were immunized twice at weekly intervals with saline or adoptively transferred NLDCs or FLDCs (1×10^5) that had been loaded in vitro with $Ova_{257–264}$ peptide (5 mice per group). DCs were incubated with 5 μM CpG for 6 hours prior to adoptive transfer immunization. At 1 week after the second immunization, mice were challenged s.c. with EG7 (3.5×10^5 cells). All of the mice immunized with antigen-loaded FLDCs were protected from tumor development, whereas control animals developed s.c. nodules within 11 days of tumor challenge ($P < 0.05$).

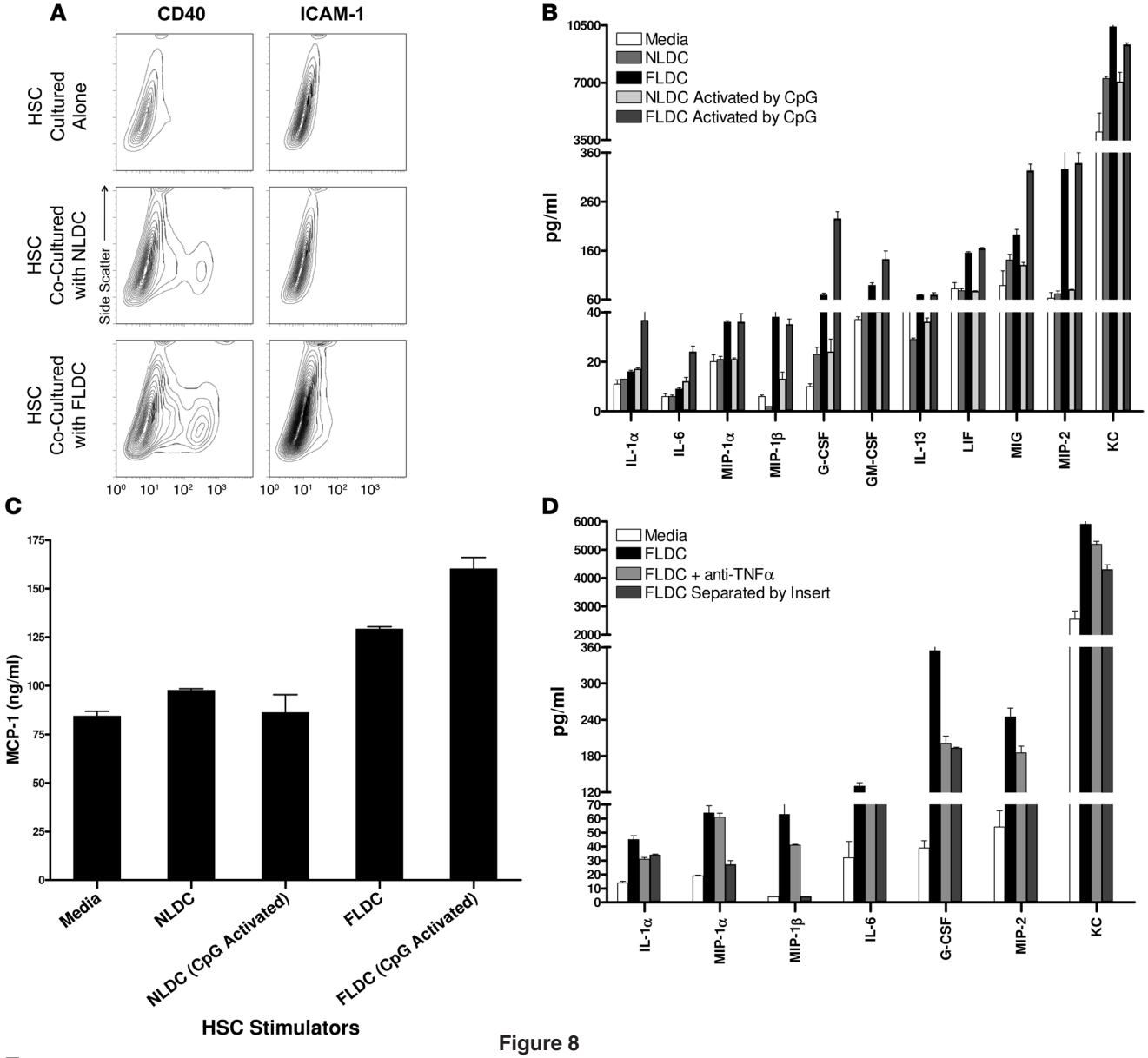

Figure 8

FLDCs activate HSCs. (**A**–**D**) HSCs were cultured alone or cocultured with DCs. At 24 hours, DCs were washed off, and HSCs were either (**A**) analyzed for surface marker expression by flow cytometry or (**B**–**D**) cultured alone for an additional 24 hours before analysis for inflammatory mediator production in conditioned media. (**A**) FLDCs induced higher HSC expression of CD40 and ICAM-1. (**B** and **C**) HSCs that had been cocultured with FLDCs produced elevated levels of numerous inflammatory mediators, whereas NLDCs only induced HSCs to produce higher KC ($P < 0.05$). Furthermore, CpG-treated FLDCs induced higher HSC production of IL-1α, IL-6, G-CSF, GMCSF, MIG, and MCP-1 compared with unstimulated FLDCs ($P < 0.05$). Conversely, priming NLDCs with CpG did not enhance their ability to activate HSCs. (**D**) To determine the mechanism of DC-HSC cross-talk, in selected experiments, cellular contact was prevented between HSCs and FLDCs by using 0.4-μm transwell inserts. Alternatively, TNF-α was blocked using 5 μg/ml 2E2. Prevention of cellular contact partially abrogated HSC production of IL-1α, MIP-1α, MIP-1β, IL-6, G-CSF, MIP-2, and KC (all $P < 0.05$). Similarly, TNF-α blockade reduced HSC production of all inflammatory mediators except MIP-1α ($P < 0.05$). (**E**) To test DC induction of HSC proliferation, irradiated DCs were coincubated with HSCs for 48 hours. Proliferation was measured by uptake of ^{3}H-thymidine over the final 12 hours. FLDCs induced a 6-fold increase in HSC proliferation ($P < 0.05$). DC-HSC experiments were repeated at least twice.

The earliest phases of liver fibrosis are regulated by a complex interplay of cytokines and chemokines. NPCs as well as parenchymal cells produce an array of inflammatory mediators that can effect direct cytotoxic tissue damage and, more critically, change the character of quiescent HSCs (8). For example, IL-6 has direct mitogenic effect on HSC proliferation in cirrhotic patients (17). MCP-1 also directly activates HSCs to deposit ECM proteins (18). Other inflammatory mediators, including IL-1α, TNF-α, IL-5, IL-13, MIP-1α, and MIP-2, have also been linked to the progression of hepatic fibro-inflammatory disease in humans and rodents (8). T cells, Kupffer cells, hepatocytes, and biliary epithelial cells have been reported to contribute to the intense inflammatory milieu in the fibrotic liver. However, to our knowledge, the role of DCs in the regulation of hepatic inflammation in liver fibrosis has not been previously studied. We showed here that DCs governed the markedly high levels of numerous inflammatory mediators by activation of neighboring cell types. One example is IFN-γ production by liver leukocytes. FLDCs mediated production of high NK cell IFN-γ production in coculture (Figures 3, C and F, and Supplemental Figure 6) as well as in vivo after FLDC adoptive transfer (Figure 4A). Similarly, CTLs generated by immunization with antigen-pulsed FLDCs secreted high levels of IFN-γ (Figure 5C). Furthermore, IFN-γ production by NPCs from fibrotic liver was abrogated after DC depletion in vitro and in vivo (Figure 2, E and F). We have not shown that DCs are essential for hepatic fibrosis itself, as effecting more than transient DC depletion in vivo is elusive. It is conceivable that fibrogenesis would proceed even in the absence of DCs. However, our data suggests that further investigations aimed at modulating DC proinflammatory function may be an attractive avenue of experimental therapeutics for reducing the inflammatory cascade in liver fibrosis, a disease for which there are few, if any, effective clinical therapies.

Another important finding in this study is that FLDCs directly activated HSCs. Although numerous cell types have been purported to interact with HSCs, including hepatocytes, liver sinusoidal endothelial cells, and Kupffer cells, to our knowledge, this is the first report of cross-talk between DCs and HSCs. We show that FLDCs induced modest upregulation of ICAM-1 and CD40 expression on HSCs (Figure 8A). Expression of ICAM-1 is upregulated following HSC activation and plays a critical role in lymphocyte adherence (19). Ligation of CD40 is associated with the initiation of inflammatory signaling pathways in HSCs (20). Furthermore, evidence of significant cross-talk between HSCs and DCs after hepatic injury is exemplified by our finding that FLDCs induced HSCs to proliferate and produce markedly elevated levels of various cytokines and chemokines (Figure 8, B–E). The results of our DC-HSC coculture experiments establish the necessity for direct DC-HSC cellular interaction for maximal activation. HSC activation by FLDCs was also partially dependent on TNF-α; however, our data suggest that additional undetermined factors are also likely responsible. The clinical significance of the robust FLDC-HSC relationship, again, may lie in the potential for therapeutic intervention in chronic liver disease by modulating DC function.

In summary, our present results show that liver DCs, which are primary contributors to hepatic tolerance in unmanipulated hosts, were conversely highly immunogenic and efficient in initiating both innate and adaptive immunity in hepatic fibrosis via a TNF-α–dependent mechanism. The phenotypically transformed DCs also controlled the proinflammatory milieu among hepatic leukocytes in liver fibrosis, as DC depletion entirely abrogated the diverse elevations in cytokines and chemokines produced by fibrotic liver NPCs. In addition, our findings also established the existence of DC-HSC cross-talk, as FLDCs transformed HSCs to a proinflammatory phenotype. Although it remains uncertain whether DCs are essential to the actual fibrotic process itself, these data deepen our understanding of liver immunology in fibro-inflammatory disease and suggest that modulation of DC biology may be an attractive approach manipulating the inflammatory cascade after hepatic insult.

Methods

Animals and fibrosis models. Male C57BL/6, BALB/c, CD45.1 (B6.SJL-*Ptprca*/BoAiTac), OT-I (B6.Cg-RAG2tm1Fwa-TgN), OT-II (B6.Cg-RAG2tm1Alt-TgN), and CD11c-DTR mice were purchased from Taconic. To induce hepatic fibrosis, mice were treated with thrice-weekly injections of TAA (250 mg/kg; Sigma-Aldrich) and leptin (1.5 mg/kg; Biomyx) for 6 weeks (21). Alternatively, mice received biweekly injections of CCl_4 (0.5 ml/kg; Sigma-Aldrich) for 12 weeks (22). In CD11c-DTR mice, transient DC depletion was accomplished with a single i.p. dose of diphtheria toxin (4 μg/kg; Sigma-Aldrich; ref. 9). Animal procedures were approved by the New York University School of Medicine IACUC.

Cellular isolation and culture. NPCs were isolated as described previously (4). The portal vein was infused with 1% collagenase IV (Sigma-Aldrich) followed by hepatectomy and mechanical digestion. Low-speed (30 *g*) centrifugation of the liver suspension was performed to exclude hepatocytes, followed by high-speed (400 *g*) centrifugation to isolate the NPCs, which were further enriched over an Optiprep (Sigma-Aldrich) gradient. DCs were purified using anti-CD11c immunomagnetic beads and passage through LS columns (Miltenyi) or FACS sorting. For HSC isolation, the liver was perfused with collagenase (1 ml/min) using a peristaltic pump. HSCs were enriched over a 3-layer Percoll (GE Healthcare) gradient (52%, 50%, and 30%; ref. 23). HSCs were used in experiments on day 14 of culture. For DC-HSC coculture assays, 5×10^5 DCs were cultured with HSCs in 24-well plates in a 1:2 ratio in complete RPMI (RPMI 1640 with 10% heat-inactivated FBS, 2 mM L-glutamine, and 0.05 mM 2-ME). In selected experiments, cellular contact was prevented using a 0.4-μm transwell insert (Costar).

Flow cytometry and cytokine analysis. Flow cytometry was performed using FACSCalibur (BD) after incubating 5×10^5 cells/tube with 1 μg anti-FcγRIII/II antibody (2.4G2, Fc block; Monoclonal Antibody Core Facility, Sloan-Kettering Institute) and then labeling with 1 μg fluorochrome-conjugated Ab (Supplemental Table 1). For cytokine analysis, cellular suspensions were cultured in complete RPMI at a concentration of 1×10^6 cells/ml for 24 hours before supernatant harvest and analysis either using either a cytometric bead array (BD) or the Milliplex Immunoassay (Millipore). Intracellular cytokine staining was performed using an intracellular cytokine detection kit according to the manufacturer's protocol (BD). In selected experiments, DCs were stimulated with TLR3 ligand Poly(I:C) (10 μg/ml), TLR4 ligand LPS (1 μg/ml), TLR5 ligand Flagellin (1 μg/ml), or TLR9 ligand CpG ODN1826 (5 μM; all from InvivoGen).

T cell and HSC proliferation assays. For in vitro T cell proliferation assays, various numbers of DCs were added to 2×10^5 allogeneic T cells, $CD8^+$OT-I TCR-transgenic T cells specific for $Ova_{257–264}$, or $CD4^+$OT-II TCR-transgenic T cells specific for $Ova_{323–339}$ in 96-well plates for 48–72 hours before pulsing with ^{3}H-thymidine as described previously (13). DCs were loaded with the relevant Ova peptide (10 μg/ml; AnaSpec) for 1 hour before use. In selected assays, TNF-α blockade using 2E2 or isotype control (5 μg/ml; Monoclonal Antibody Core Facility, Sloan-Kettering Institute) were used. To assess $CD4^+$ T cell priming in regional lymph nodes, $CD45.1^+$ mice were administered an i.v. injection of 2×10^6 $CD45.2^+$OT-II splenic T cells. At 18 hours, mice received a footpad immunization with 2×10^5 DC.$Ova_{323–339}$.

At 90 hours, ipsilateral popliteal lymph nodes were harvested, and the number of $CD3^+CD4^+CD45.2^+$ T cells was measured by flow cytometry. To evaluate intrahepatic $CD8^+$ T cell proliferation in vivo, C57BL/6 mice were administered an i.v. injection of 2×10^6 OT-I splenic T cells followed 18 hours later by an i.v. injection of 2×10^5 DC.$Ova_{257-264}$ or Ova (1 mg; Sigma-Aldrich). $CD8^+$ T cell proliferation in the liver was determined by measuring the number of hepatic $CD3^+CD8^+Ova_{257-264}Pentramer^+$ cells (ProImmune). For HSC proliferation assays, 2×10^4 HSCs were cultured for 2 days in 48-well dishes, either alone or with 1×10^5 irradiated (30 Gy) liver DCs. For the last 12 hours of coculture, cells were pulsed with ^{3}H-thymidine, and proliferation was measured using a MicroBeta scintillation counter (Perkin Elmer).

CTL assays and tumor experiments. Mice were immunized with DC.$Ova_{257-264}$ (1×10^5) twice at weekly intervals. For CTL assays, 1 week after the second immunization, splenocytes from immunized animals were harvested, restimulated with $Ova_{257-264}$ peptide (10 μg/ml) for 5 days, and then tested against 1×10^4 ^{51}Cr-labeled EG7 cells (ATCC) in various E/T ratios. For tumor experiments, 1 week after the second immunization, mice were challenged s.c. with 3×10^5 EG7 cells.

NK cell assays. DC-NK cocultures were performed as described previously (13). Briefly, 1×10^5 splenic NK cells were plated with 2×10^5 DCs in 96-well plates for 18–24 hours. For cytotoxicity assays, NK cells were repurified using immunomagnetic beads and plated against 2×10^3 ^{51}Cr-labeled Yac-1 targets (ATCC). For in vivo NK stimulation assays, 1×10^5 DCs were adoptively transferred to mice by direct splenic inoculation via flank laparotomy. At 18 hours, splenic NK cells were harvested for analysis.

Histology and immunofluorescence. For histological analysis, livers were fixed with 10% buffered formalin, dehydrated in ethanol, embedded with paraffin, and stained with H&E, Masson trichrome, or picric acid–Sirius red. For immunofluorescence studies, frozen sections of liver were stained with anti-CD11c (BD). Images were captured on an Axiovert 200M fluorescence microscope (Zeiss).

Statistics. Data are presented as mean ± SEM, representing replicates within an experiment. Survival was measured according to the Kaplan-Meier method. Statistical significance was determined by the Student's *t* test and the log-rank test using 2-tailed analysis. A *P* value less than 0.05 was considered significant.

Acknowledgments

The authors thank Scott Friedman (Mount Sinai School of Medicine, New York, New York, USA) and his laboratory for instruction in the isolation and culture of HSCs. This work was supported in part by a Liver Scholar Award from the American Liver Foundation (to G. Miller), a Whitehead Fellowship Award for Junior Faculty in Biomedical and Biological Sciences (to G. Miller), and NIH awards F30 AA 017344-01 (to J. Mallen-St. Clair), CA55360-18 (to D. Bar-Sagi), and CA108573 (to A.B. Frey).

Received for publication June 26, 2009, and accepted in revised form August 26, 2009.

Address correspondence to: George Miller, Departments of Surgery and Cell Biology, New York University School of Medicine, Medical Science Building 626, 550 First Avenue, New York, New York 10016, USA. Phone: (212) 263-0570; Fax: (212) 263-6840; E-mail: george.miller@nyumc.org.

1. Goubier, A., et al. 2008. Plasmacytoid dendritic cells mediate oral tolerance. *Immunity.* **29**:464–475.
2. Tokita, D., et al. 2008. Poor allostimulatory function of liver plasmacytoid DC is associated with pro-apoptotic activity, dependent on regulatory T cells. *J. Hepatol.* **49**:1008–1018.
3. Xia, S., et al. 2008. Hepatic microenvironment programs hematopoietic progenitor differentiation into regulatory dendritic cells maintaining liver tolerance. *Blood.* **112**:3175–3185.
4. Pillarisetty, V.G., Shah, A.B., Miller, G., Bleier, J.I., and DeMatteo, R.P. 2004. Liver dendritic cells are less immunogenic than spleen dendritic cells because of differences in subtype composition. *J. Immunol.* **172**:1009–1017.
5. Jeong, W.I., and Gao, B. 2008. Innate immunity and alcoholic liver fibrosis. *J. Gastroenterol. Hepatol.* **23**(Suppl. 1):S112–S118.
6. Kita, H., et al. 2002. Identification of HLA-A2-restricted CD8(+) cytotoxic T cell responses in primary biliary cirrhosis: T cell activation is augmented by immune complexes cross-presented by dendritic cells. *J. Exp. Med.* **195**:113–123.
7. Seki, E., et al. 2009. CCR1 and CCR5 promote hepatic fibrosis in mice. *J. Clin. Invest.* **119**:1858–1870.
8. Wynn, T.A. 2008. Cellular and molecular mechanisms of fibrosis. *J. Pathol.* **214**:199–210.
9. Plitas, G., et al. 2008. Dendritic cells are required for effective cross-presentation in the murine liver. *Hepatology.* **47**:1343–1351.
10. Bahcecioglu, I.H., et al. 2008. Hepatoprotective effect of infliximab, an anti-TNF-alpha agent, on carbon tetrachloride-induced hepatic fibrosis. *Inflammation.* **31**:215–221.
11. Natsume, M., et al. 1999. Attenuated liver fibrosis and depressed serum albumin levels in carbon tetrachloride-treated IL-6-deficient mice. *J. Leukoc. Biol.* **66**:601–608.
12. Bataller, R., and Brenner, D.A. 2005. Liver fibrosis. *J. Clin. Invest.* **115**:209–218.
13. Miller, G., et al. 2002. Endogenous granulocyte-macrophage colony-stimulating factor overexpression in vivo results in the long-term recruitment of a distinct dendritic cell population with enhanced immunostimulatory function. *J. Immunol.* **169**:2875–2885.
14. Bamboat, Z.M., et al. 2009. Human liver dendritic cells promote T cell hyporesponsiveness. *J. Immunol.* **182**:1901–1911.
15. O'Beirne, J., Mitchell, J., Farzaneh, F., and Harrison, P.M. 2009. Inhibition of major histocompatibility complex Class I antigen presentation by hepatitis C virus core protein in myeloid dendritic cells. *Virology.* **389**:1–7.
16. Xie, Q., et al. 2009. Patients with chronic hepatitis B infection display deficiency of plasmacytoid dendritic cells with reduced expression of TLR9. *Microbes Infect.* **11**:515–523.
17. Toda, K., et al. 2000. Induction of hepatic stellate cell proliferation by LPS-stimulated peripheral blood mononuclear cells from patients with liver cirrhosis. *J. Gastroenterol.* **35**:214–220.
18. Marra, F., et al. 1999. Monocyte chemotactic protein-1 as a chemoattractant for human hepatic stellate cells. *Hepatology.* **29**:140–148.
19. Hellerbrand, C., Wang, S.C., Tsukamoto, H., Brenner, D.A., and Rippe, R.A. 1996. Expression of intracellular adhesion molecule 1 by activated hepatic stellate cells. *Hepatology.* **24**:670–676.
20. Schwabe, R.F., Schnabl, B., Kweon, Y.O., and Brenner, D.A. 2001. CD40 activates NF-kappa B and c-Jun N-terminal kinase and enhances chemokine secretion on activated human hepatic stellate cells. *J. Immunol.* **166**:6812–6819.
21. Dai, K., Qi, J.Y., and Tian, D.Y. 2005. Leptin administration exacerbates thioacetamide-induced liver fibrosis in mice. *World J. Gastroenterol.* **11**:4822–4826.
22. Louis, H., et al. 1998. Interleukin-10 controls neutrophilic infiltration, hepatocyte proliferation, and liver fibrosis induced by carbon tetrachloride in mice. *Hepatology.* **28**:1607–1615.
23. Vrochides, D., Papanikolaou, V., Pertoft, H., Antoniades, A.A., and Heldin, P. 1996. Biosynthesis and degradation of hyaluronan by nonparenchymal liver cells during liver regeneration. *Hepatology.* **23**:1650–1655.